FACTA UNIVERSITATIS
Series: **Mechanical Engineering** Vol. 22, Nº 4, 2024, pp. 673 - 688
https://doi.org/10.22190/FUME240904048N

Original scientific paper

ANALYSIS OF NANOBEAM-BASED MICROSTRUCTURE IN N/MEMS SYSTEM USING VAN DER WAALS FORCES

Muhammad Nadeem[1], Qura-Tul Ain[2], Naif Almakayeel[3], Yabin Shao[4], Shuqiang Wang[5], Meshal Shutaywi[6]

[1]School of Mathematics and Statistics, Qujing Normal University, Qujing China
[2]Institute of Computing Science and Technology, Guangzhou University, Guangzhou, China
[3]Department of Industrial Engineering, College of Engineering, King Khalid University, Abha, Saudi Arabia
[4]Research Institute of Microscale Optoelectronics, School of Jia Yang, Zhejiang Shuren University, Shaoxing China
[5]Shenzhen Institutes of Advanced Technology, Chinese Academy of Sciences
[6]Department of Mathematics, College of Science & Arts, King Abdul Aziz University, Rabigh, Saudi Arabia

ORCID iDs: Muhammad Nadeem https://orcid.org/0000-0002-9349-4729
Qura-Tul Ain https://orcid.org/0000-0003-4442-4756
Naif Almakayeel https://orcid.org/0000-0001-9461-5935
Yabin Shao https://orcid.org/0009-0003-1925-9231
Shuqiang Wang https://orcid.org/0000-0003-1119-320X
Meshal Shutaywi https://orcid.org/0000-0003-1454-2962

Abstract. *Nano/microelectromechanical system (N/MEMS) have garnered significant global attention for their transformative applications across various cutting-edge fields, including wearable devices, 5G service, collecting power, and space travel. These systems face challenges when exposed to excessive forces and leading to pull-in instability that can undermine a reliable performance. Therefore, it is essential to quickly and precisely comprehend the periodic motion of the system to minimize the possibility of pull-in instability and maintain consistent operation. This article explores the application of the homotopy transformation scheme (HTS) for forecasting dynamic behavior of N/MEMS. The most advantage of HTS is its ability to deliver results without relying on hypotheses, assumptions, or constraints on variables. To illustrate its effectiveness, we use a generalized N/MEMS oscillator system, presenting an accurate analysis of analytic solution. Specifically, we focus on a microstructure of nanobeam-based system actuated by van der Waals (vdW) forces to highlight its periodic characteristics. The results reveal that HTS provides a robust comparison and excellent agreement with the exact solution, underscoring its reliability and precision.*

Key words: *Sumudu transform, N/MEMS, Homotopy perturbation method, Approximate solution*

Received: September 04, 2024 / Accepted November 17, 2024
Corresponding author: Yabin Shao
Zhejiang Shuren University, Shaoxing 312028 China
E-mail: shaoyabin@zjsru.edu.cn (Shao)

1. INTRODUCTION

Nano/microelectromechanical systems (N/MEMSS) represents a cutting-edge technology characterized by their exceptional geometrical precision, reliable performance, and high sensitivity. These systems achieved various advanced properties through meticulous control of applied voltage and involved both fixed and dynamic elements; whenever an effort is exerted for activation [1, 2]. The N/MEMS have a variety of potential areas, consisting of wearable instruments, 5G service, and collecting power [3-6]. The transformative impact of these systems on various technologies has prompted extensive research into their operational properties and potential applications. Recent advancements in nanotechnology have brought significant attention to the dynamic issues of nanotubes within nanostructures and systems. Size-dependent behavior in clamped-clamped microbeam systems has important mechanical and structural responses due to the change in beam dimensions at the microscale level. Small-scale clamped-clamped beams may display nonlinear behavior, particularly at significant deflections or when subjected to electrostatic forces in MEMS systems. Nonlinear components emerge as importance in dealing with problems, influencing frequency and equilibrium, and providing size-dependent nonlinearity [7, 8]. Researchers have found that oscillators in N/MEMS exhibit complex dynamics, such as pull-in instability, phase diagrams, and hysteresis being crucial to their dynamic analysis [9, 10]. The basic mode of oscillation coincides with the main stretching of the beam. The ends are fixed for a doubly clamped beam, thus its initial frequency is higher than that of simply supported or free ends. This fixed structure enhances elasticity, which implies that the beam needs more energy to oscillate, and raises the fundamental frequency. Nonlinear oscillatory dynamics are often utilized in energy-harvesting instances, in which the oscillations of the beam transform mechanical power to electrical power. Subsequently, damping and harmonic stability are essential for performance. The criteria for the existence of periodic solutions and their associated properties are crucial for the efficiency and aesthetics of nanotube-based N/MEMS and resonators [11-13].

The Casimir effect arises from quantum fluctuations and can be viewed as an attractive force between conducting plates; nevertheless, it comes from the same fundamental principles that govern vdW interactions. The vdW force originates from the relationships across temporary dipoles induced by electron density fluctuations within molecules. This force is applicable to all molecules, irrespective of their features. This indicates that even though the plates are formed of nonpolar objects, the vdW force remains present. This force becomes crucial in influencing the system's behavior when the plates are close together. In recent years, various researchers have particularly focused to overcome the difficulty of obtaining analytical solution for N/MEMS system. These solutions provide fruitful insights that are vital for comprehensive understanding of the behavior and characteristics of these advanced systems. Most of the numerical methods often fail to explicitly capture the nonlinear frequency amplitude relationship. As a result, various analytical methods have been developed in the literature to address N/MEMS oscillators. These methods include the variational iteration approach [14], energy balance technique [15], iteration perturbation scheme [16], residual harmonic balance strategy [17], parameter expansion approach [18], Adomian decomposition technique [19], power series [20], He-transform [21], and frequency formulation [22].

The homotopy perturbation method (HPM) is an extremely successful tool for the resolution of a diverse array of nonlinear problems. This method involves expressing the outcomes as a sequence that swiftly turns to precise results. A standout feature of HPM is

its ability to achieve high accuracy with just a single iteration. This characteristic significantly enhances its appeal and practicality in numerous fields of technology and scientific research. Pull-in instability exhibits significant nonlinearity as a result of the inverse-square relationship of electrostatic forces relative to the gap distance. Nonlinear behaviors demand iterative and perturbation techniques to identify the crucial points related to instability. Consequently, HPM provides a feasible analytical method for deriving approximation solutions [23]. Qayyum and Oscar [24] proposed the least square homotopy perturbation approach to analyze multiple order problems related to boundary values. Anjum and He [25] studied the nonlinear vibration properties of nanotube-based N/MEMS oscillators using the HPM and the Laplace transform. HPM has been widely regarded as an auspicious and innovative approach for addressing nonlinear problems [26-28]. On the other hand, the Sumudu transform [29] is a mathematical tool used to simplify the analysis of differential equations. It simplifies the solution of differential problems by converting them into an algebraic formula. It is highly effective in handling with initial value problems and certain types of nonlinear problems [30, 31].

In this work, we design the homotopy transformation scheme (HTS) through the association of Sumudu transform and the homotopy perturbation method. This technique is straightforward to utilize for nonlinear differential problems. Using this scheme, we can obtain the results of the N/MEMS system in the form of a convergent series. We focus on the solution of nonlinear behavior of dynamic oscillatory for doubly clamped nanobeam that is controlled and governed by vdW forces. We evaluate the outcomes of HTS by comparing them to the derived results via some mathematical software by utilizing the R-K method of 4th order and other established schemes.

2. Basic Idea of Sumudu Transformation

Let A be the set of function, which is defined as [32]:

$$A = \vartheta(t):\ \exists\, \mathrm{M}, r_1, r_2 > 0, |\vartheta(t)| < Me^{\frac{|t|}{r_j}}, if\ \ t \in (-1)^j \times [0,\infty). \tag{1}$$

For every function in the set A, it is necessary for the constant M to be a finite number, whereas the constants r_1 and r_2 may be either finite or infinite. Furthermore, the Sumudu transform is defined as an integral equation such that

$$\mathbb{S}\left[\vartheta(t)\right] = R(\theta) = \int_0^\infty \vartheta(\theta t)e^{-t}dt = \frac{1}{\theta}\int_0^\infty \vartheta(t)e^{-\frac{t}{\theta}}dt, \quad t \geq 0, \tag{2}$$

where θ is an independent of t parameter that might be real or complex. The inversion expression for ST is as follows

$$\mathbb{S}\left[R(\theta)\right] = \frac{1}{2\Pi i}\int_{a-i\infty}^{a+i\infty} e^{\theta t}R\left(\frac{1}{\theta}\right)\frac{d\theta}{\theta}. \tag{3}$$

The subsequent characteristics are beneficial in the calculations of Sumudu space.

$$\begin{aligned}
&\mathbb{S}\left[t^n\right] = n!\theta^n, \quad n \in \mathbb{N},\\
&\mathbb{S}\left[\vartheta'(t)\right] = \frac{R(\theta)}{\theta} - \frac{\vartheta(0)}{\theta},\\
&\mathbb{S}\left[\vartheta''(t)\right] = \frac{R(\theta)}{\theta^2} - \frac{\vartheta(0)}{\theta^2} - \frac{\vartheta'(0)}{\theta},\\
&\mathbb{S}\left[\vartheta^n(t)\right] = \frac{R(\theta)}{\theta^n} - \frac{\vartheta(0)}{\theta^n} - \ldots - \frac{\vartheta^{n-1}(0)}{\theta}.
\end{aligned} \tag{4}$$

We introduce these properties during the development of HTS so that our proposed scheme can provide accurate results.

3. Development of Homotopy Transformation Scheme

Here, we propose the development of HTS for a general problem. We explain the step-by-step formulation of proposed scheme. We show the process of handling the nonlinear terms and derived a series result by using the application of HPM. This obtained series can easily converge to the exact results only after a few steps of series. Let us examine the process of HTS by starting a nonlinear fractional differential problem such as,

$$\frac{d^2\vartheta}{dt^2} + f(\vartheta) = r(t), \tag{5}$$

with following constraints

$$\vartheta(0) = B, \quad \vartheta'(0) = 0. \tag{6}$$

Eq. (5) can be modified in the following manner:

$$\frac{d^2\vartheta}{dt^2} + \omega^2\vartheta + g(\vartheta) = r(t), \tag{7}$$

where $g(\vartheta)=f(\vartheta)-\omega^2\vartheta$. Let us define the term $g(\vartheta)$ such as

$$\frac{d^2\vartheta}{dt^2} + \omega^2\vartheta + L_1 g(\vartheta) + L_2 g(\vartheta) = r(t), \tag{8}$$

in which L_1 be linear and L_2 is a nonlinear operator with a source parameter $r(t)$. Operating the linearity of ST to Eq. (8), we can write it as follows:

$$\frac{R(\theta)}{\theta^2} - \frac{\vartheta(0)}{\theta^2} - \frac{\vartheta'(0)}{\theta} + \omega^2 R(\theta) + \mathbb{S}\left[L_1 g(\vartheta) + L_2 g(\vartheta)\right] = \mathbb{S}\left[r(t)\right]. \tag{9}$$

Using condition of Eq. (6), we can simplify it to obtain $R(\theta)$ such as

$$R(\theta) = \frac{B}{(1+\theta^2\omega^2)} - \frac{\theta^2}{(1+\theta^2\omega^2)}\mathbb{S}[L_1 g(\vartheta) + L_2 g(\vartheta)] + \frac{\theta^2}{(1+\theta^2\omega^2)}\mathbb{S}[r(t)]. \tag{10}$$

Now, using the property of inverse ST on Eq. (10), we get

$$\vartheta(t) = B\cos\omega t - \mathbb{S}^{-1}\left[\frac{\theta^2}{(1+\theta^2\omega^2)}\mathbb{S}[L_1 g(\vartheta) + L_2 g(\vartheta)]\right] + \mathbb{S}^{-1}\left[\frac{\theta^2}{(1+\theta^2\omega^2)}\mathbb{S}[r(t)]\right], \tag{11}$$

we can also write it as follows

$$\vartheta(t) = G(t) - \mathbb{S}^{-1}\left[\frac{\theta^2}{(1+\theta^2\omega^2)}\mathbb{S}[L_1 g(\vartheta) + L_2 g(\vartheta)]\right], \tag{12}$$

where

$$G(t) = B\cos\omega t + \mathbb{S}^{-1}\left[\frac{\theta^2}{(1+\theta^2\omega^2)}\mathbb{S}\left[r(t)\right]\right]. \tag{13}$$

Let the general expression of Eq. (12) is

$$\vartheta(t) = \sum_{n=0}^{\infty} p^n \vartheta_n(t). \tag{14}$$

We introduce the concept of HPM to decompose the terms of nonlinear operator L_2 in Eq. (12) such as

$$L_2 g(\vartheta) = \sum_{n=0}^{\infty} p^n H_n(\vartheta), \tag{15}$$

with $p \in [0,1]$ as a small term of perturbation and $H_n(\vartheta)$ represents the He's polynomials that are produced by the following formula

$$H_n(\vartheta) = H_n(\vartheta_0, \vartheta_1, \ldots, \vartheta_n) = \frac{1}{n!}\frac{\partial^n}{\partial p^n}\left(L_2 g\left(\sum_{i=0}^{\infty} p^n \vartheta_i\right)\right)_{p=0}, \quad n = 0,1,2,\ldots \tag{16}$$

On utilizing Eqs. (14) and (15) to Eq. (12), we can obtain such as

$$\sum_{n=0}^{\infty} p^n \vartheta_n(t) = G(t) - p\left(\mathbb{S}^{-1}\left[\frac{\theta^2}{(1+\theta^2\omega^2)}\mathbb{S}[L_1 \sum_{n=0}^{\infty} p^n g(\vartheta_n) + \sum_{n=0}^{\infty} p^n H_n]\right]\right). \tag{17}$$

After some successive repetitions along with the analysis of components p, we construct the following results:

$$\begin{aligned}
&p^0 = \vartheta_0(t) = G(t),\\
&p^1 = \vartheta_1(t) = -\mathbb{S}^{-1}\left[\frac{\theta^2}{1+\theta^2\omega^2}\mathbb{S}\left\{L_1 g(\vartheta_0) + H_0(\vartheta)\right\}\right],\\
&p^2 = \vartheta_2(t) = -\mathbb{S}^{-1}\left[\frac{\theta^2}{1+\theta^2\omega^2}\mathbb{S}\left\{L_1 g(\vartheta_1) + H_1(\vartheta)\right\}\right],\\
&\vdots\\
&p^n = \vartheta_n(t) = -\mathbb{S}^{-1}\left[\frac{\theta^2}{1+\theta^2\omega^2}\mathbb{S}\left\{L_1 g(\vartheta_{n-1}) + H_{n-1}(\vartheta)\right\}\right].
\end{aligned} \tag{18}$$

Finally, the above series can be expressed as follows:

$$\vartheta(t) = \vartheta_0 + \vartheta_1 + \vartheta_2 + \ldots = \lim_{p\to\infty} \sum_{i=0}^{\infty} \vartheta_i(t). \tag{19}$$

This approach efficiently utilizes the principle of continuous iteration and mathematical investigation to reveal an extensive solution for the proposed model, and effectively demonstrates the ability of HTS procedures to address intricate problems.

4. PROBLEM FORMULATION

Nanobeams serve as the primary structural components in N/MEMS systems and play a crucial role in their functionality. To effectively analyze the behavior of these beams, various beam theories are employed. These theories not only facilitate the analysis of beam behavior but also enhance the design process that ensures the development of robust and high-performing N/MEMS system. Consider a nanobeam with clamped-clamped boundary conditions as shown in Fig. 1, where L is the length between the two clamped ends of the beam, b is the width of the beam in the plane perpendicular to its length, h shows the thickness of the beam in the plane perpendicular to its width and length, and ρ is the mass per unit volume of the material of the beam.

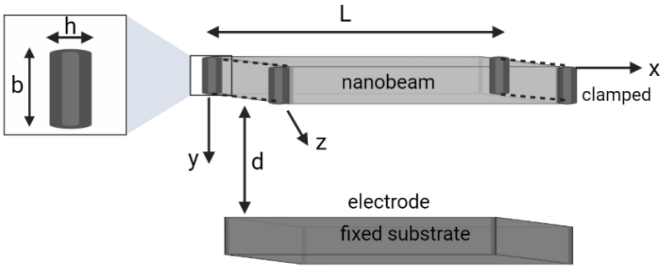

Fig. 1 Schematics of a double-sided driven clamped-clamped microbeam

This study delves into the dynamic behavior and properties of such a nanobeam structure that focusing on its transverse vibrations and the resulting mode shapes and natural frequencies. By leveraging the Euler-Bernoulli beam theory and applying the appropriate boundary conditions, our purpose is to demonstrate a comprehensive analysis of the mechanical response of the nanobeam under various conditions. This investigation is essential for applications where precise control and understanding of nanoscale mechanical elements are required. Consider the von-Karman nonlinearity for mid-plane stretching, depending on the Euler-Bernoulli beam idea as follows:

$$EI\frac{\partial^4 Q}{\partial \psi^4} + \rho S\frac{\partial^2 Q}{\partial \eta^2} - \left[N + \frac{ES}{2L}\int_0^L \left(\frac{\partial Q}{\partial \psi}\right)^2 d\psi \right] \frac{\partial^2 Q}{\partial \psi^2} - K(\psi,\eta) = 0, \tag{20}$$

where Q is a function of ψ and η that indicates the spatial location and time respectively, E denotes the effective Young's modulus of the beam, while I indicate the moment of inertia

about the cross-section of *y*-axis. Additionally, $\tilde{N}$ signifies the residual axial load. The function $K(\psi, \eta)$ describes the vdW forces among nanobeam and the substrate and is stated as follows [33]:

$$K(\psi,\eta)=\frac{A_h b}{6\Pi(d-Q)^3}, \tag{21}$$

where A_h denotes the Hamaker coefficient with a value of $30 \times 10^{-19}\, J < A_h < 50 \times 10^{-19}\, J$, $S=bh$, whereas d shows the distance among nanobeam and the substrate. We can define the nondimensional parameters as follows:

$$\varphi=\frac{\psi}{L},\ \delta=\frac{Q}{d},\ t=\frac{\eta}{T}, \tag{22}$$

where

$$T=\sqrt{\frac{\rho h b L^4}{EI}}. \tag{23}$$

Employing the value of Eq. (22) into Eq. (20), we can obtain the following form

$$\frac{\partial^4\delta}{\partial\varphi^4}+\frac{\partial^4\delta}{\partial t^2}-\left[N+\alpha\int_0^1\left(\frac{\partial\delta}{\partial\varphi}\right)^2 d\varphi\right]\frac{\partial^2\delta}{\partial\varphi^2}-\frac{\lambda}{(1-\delta)^3}=0, \tag{24}$$

where N is the load of axial, α shows the aspect ratio, whereas λ is the van der Waals force such that:

$$N=\frac{NL^2}{EI},\ \alpha=6\left(\frac{d}{h}\right)^2,\ \lambda=\frac{12A_h}{Eh^3}\left(\frac{L}{d}\right)^4. \tag{25}$$

Moreover, we have the dimensionless boundary conditions, which are stated as below

$$\delta(0,t)=\delta(1,t)=0,\quad \left.\frac{\partial\delta}{\partial\varphi}\right|_{(0,t)}=\left.\frac{\partial\delta}{\partial\varphi}\right|_{(1,t)}=0. \tag{26}$$

Since the singularity in Eq. (24) renders it challenging to resolve when $\delta=1$. Therefore, we consider the separation of variables approach to minimize Eq. (24) to an ordinary differential equation, such that $\delta(\varphi,t)$ be the result of two distinct functions as follows:

$$\delta(\varphi,t)=\varsigma(\varphi)\vartheta(t), \tag{27}$$

here $\vartheta(t)$ is a time-dependent function and $\varsigma(\varphi)$ denotes the first mode shape function that fulfills the boundary criteria. Putting the value of Eq. (27) into Eq. (24), and then multiplying the result with $\varsigma(\varphi)(1\text{-}\delta)^3$ and taking integration over the dimensionless domain, we derive

$$\begin{aligned}&\int_0^1\varsigma(1-\varsigma\vartheta)^3\vartheta\frac{\partial^4\varsigma}{\partial\varphi^4}d\varphi+\int_0^1\varsigma^2(1-\varsigma\vartheta)^3\frac{\partial^2\vartheta}{\partial t^2}d\varphi-\\&\int_0^1\varsigma(1-\varsigma\vartheta)^3\left[N+\alpha\int_0^1\left(\frac{\partial\delta}{\partial\varphi}\right)^2 d\varphi\right]\vartheta\frac{\partial^2\varsigma}{\partial\varphi^2}d\varphi-\int_0^1\lambda\varsigma d\varphi=0,\end{aligned} \tag{28}$$

which may turn to the following form:

$$(q_0 + q_1\vartheta + q_2\vartheta^2 + q_3\vartheta^3)\frac{d^2\vartheta}{dt^2} + q_4 + q_5\vartheta + q_6\vartheta^2 + q_7\vartheta^3 + q_8\vartheta^4 + q_9\vartheta^5 + q_{10}\vartheta^6 = 0, \quad (29)$$

here, the expression of $q_j(j=0,1,2,3,\ldots,10)$ is defined in the Appendix. The Eq. (29) has the following initial conditions such that

$$\vartheta(0) = B, \qquad \vartheta_t(0) = 0. \quad (30)$$

Since Eq. (29) is extremely nonlinear, thus it was difficult to solve using several well-known analytical techniques [34-36]. Thus, we construct HTS to solve Eq. (29) with the initial conditions of Eq. (30).

5. Application of Homotopy Transformation Scheme for N/MEMS

In the following part, we construct the formulation of HTS for the nanobeam-based microstructure system actuated by van der Waals forces. Therefore:

$$(q_0 + q_1\vartheta + q_2\vartheta^2 + q_3\vartheta^3)\frac{d^2\vartheta}{dt^2} + q_4 + q_5\vartheta + q_6\vartheta^2 + q_7\vartheta^3 + q_8\vartheta^4 + q_9\vartheta^5 + q_{10}\vartheta^6 = 0. \quad (31)$$

Dividing Eq. (31) by q_0, we get

$$\frac{d^2\vartheta}{dt^2} + \omega^2\vartheta + g(\vartheta) = 0, \quad (32)$$

where

$$g(\vartheta) = (d_1\vartheta + d_2\vartheta^2 + d_3\vartheta^3)\frac{d^2\vartheta}{dt^2} + d_4 + (d_5 - \omega^2)\vartheta + d_6\vartheta^2 + d_7\vartheta^3 + d_8\vartheta^4 + d_9\vartheta^5 + d_{10}\vartheta^6. \quad (33)$$

Utilizing the idea of ST on both sides of Eq. (32), we have

$$\frac{R(\theta)}{\theta^2} - \frac{B}{\theta^2} + \omega^2 R(\theta) + \mathbb{S}[\Omega] = 0. \quad (34)$$

where

$$\Omega = (d_1\vartheta + d_2\vartheta^2 + d_3\vartheta^3)\frac{d^2\vartheta}{dt^2} + d_4 + (d_5 - \omega^2)\vartheta + d_6\vartheta^2 + d_7\vartheta^3 + d_8\vartheta^4 + d_9\vartheta^5 + d_{10}\vartheta^6. \quad (35)$$

We can simplify it to obtain $R(\theta)$ such as

$$R(\theta) = \frac{B}{1+\theta^2\omega^2} - \frac{\theta^2}{1+\theta^2\omega^2}\mathbb{S}[\Omega]. \quad (36)$$

Now, using the property of inverse ST, we get

$$\vartheta(t) = B\cos\omega t - \mathbb{S}^{-1}\left[\frac{\theta^2}{1+\theta^2\omega^2}\mathbb{S}\{\Omega\}\right]. \quad (37)$$

Let the general expression of Eq. (32) is

$$\vartheta(t) = \sum_{n=0}^{\infty} p^n \vartheta_n(t). \tag{38}$$

Using the idea of HPM, we obtain Eq. (37) as follows:

$$\sum_{n=0}^{\infty} p^n \vartheta_n(t) = B\cos\omega\, t - p\left(\mathbb{S}^{-1}\left[\frac{\theta^2}{1+\theta^2\omega^2}\mathbb{S}\left\{(d_5-\omega^2)\sum_{n=0}^{\infty} p^n\vartheta_n + \sum_{n=0}^{\infty} p^n H_n\right\}\right]\right). \tag{39}$$

On comparing the components p, we construct the following results:

$$\begin{aligned} p^0 &= \vartheta_0 = B\cos\omega\, t, \\ p^1 &= \vartheta_1 = -\mathbb{S}^{-1}\left[\frac{\theta^2}{1+\theta^2\omega^2}\mathbb{S}\{\Omega\}\right], \\ &\vdots \end{aligned} \tag{40}$$

The above equation can also be written as

$$\begin{aligned} \vartheta_1 = -\mathbb{S}^{-1}&\left[\frac{\theta^2}{1+\theta^2\omega^2}\mathbb{S}\{\Gamma_0 + \Gamma_1\cos\omega\, t + \Gamma_2\cos 2\omega\, t + \Gamma_3\cos 3\omega\, t\}\right] \\ &\mathbb{S}^{-1}\left[\frac{\theta^2}{1+\theta^2\omega^2}\mathbb{S}\{\Gamma_4\cos 4\omega\, t + \Gamma_5\cos 5\omega\, t + \Gamma_6\cos 6\omega\, t\}\right] \end{aligned} \tag{41}$$

where the coefficients Γ_n (n=0,1,2, 3,...,6) can be evaluated as

$$\begin{aligned} \Gamma_0 &= -B\omega^2\left(\frac{d_1 B}{2} + \frac{3d_3B^3}{8}\right) + d_4 + \frac{d_6B^2}{2} + \frac{3d_8B^4}{8} + \frac{5d_{10}B^6}{16}, \\ \Gamma_1 &= -B\omega^2\left(1 + \frac{3d_2B^2}{4}\right) + Bd_5 + \frac{3d_7B^3}{4} + \frac{5d_9B^5}{8}, \\ \Gamma_2 &= -B\omega^2\left(\frac{d_1B}{2} + \frac{d_3B^3}{2}\right) + \frac{d_6B^2}{2} + \frac{d_8B^4}{2} + \frac{15d_{10}B^6}{32}, \\ \Gamma_3 &= -B\omega^2\left(\frac{d_2B^2}{4}\right) + \frac{d_7B^3}{4} + \frac{5d_9B^5}{16}, \\ \Gamma_4 &= -B\omega^2\left(\frac{d_3B^3}{8}\right) + \frac{d_8B^4}{8} + \frac{3d_{10}B^6}{16}, \\ \Gamma_5 &= \frac{d_9B^5}{16}, \\ \Gamma_6 &= \frac{d_{10}B^6}{32}. \end{aligned} \tag{42}$$

After adopting inverse ST to resolve Eq. (41), we obtain the following:

$$\begin{aligned}\vartheta_1 &= \frac{\Gamma_0}{\omega^2}(\cos\omega\, t-1)-\frac{\Gamma_1}{2\omega}t\sin\omega\, t-\frac{\Gamma_2}{3\omega^2}(\cos\omega\, t-\cos 2\omega\, t)\\ &-\frac{\Gamma_3}{8\omega^2}(\cos\omega\, t-\cos 3\omega\, t)-\frac{\Gamma_4}{15\omega^2}(\cos\omega\, t-\cos 4\omega\, t)\\ &-\frac{\Gamma_5}{24\omega^2}(\cos\omega\, t-\cos 5\omega\, t)-\frac{\Gamma_6}{35\omega^2}(\cos\omega\, t-\cos 6\omega\, t).\end{aligned} \tag{43}$$

In order to preserve its periodicity for the system, the components of $t\sin\omega\, t$ must be zero. Consequently,

$$\frac{\Gamma_1}{2\omega}=0, \tag{44}$$

or

$$-B\omega^2\left(1+\frac{3d_2B^2}{4}\right)+Bd_5+\frac{3d_7B^3}{4}+\frac{5d_9B^5}{8}=0. \tag{45}$$

It produces the following result:

$$\omega=\sqrt{\frac{8d_5+6d_7B^2+5d_5B^4}{8+6d_2B^2}}, \tag{46}$$

Subsequently, the estimated first-order analytical result is as follows:

$$\begin{aligned}\vartheta_{HTS} &= a_0+(a_1+B)\cos\omega\, t+a_2\cos 2\omega\, t\\ &+a_3\cos 3\omega\, t+a_4\cos 4\omega\, t+a_5\cos 5\omega\, t+a_6\cos 6\omega\, t,\end{aligned} \tag{47}$$

Therefore, using Eqs. (46) and (47), we can derive the periodic motion of doubly clamped N/MEMS system built on nanobeams with vdW forces, and where:

$$\begin{aligned}&a_0=-\frac{\Gamma_0}{\omega^2},\ \ a_1=\frac{1}{\omega^2}\left(\Gamma_0-\frac{\Gamma_2}{3}-\frac{\Gamma_3}{8}-\frac{\Gamma_4}{15}-\frac{\Gamma_5}{24}-\frac{\Gamma_6}{35}-\frac{\Gamma_7}{48}\right),\ \ a_2=\frac{\Gamma_2}{3\omega^2},\\ &a_3=\frac{\Gamma_3}{8\omega^2},\ \ a_4=\frac{\Gamma_4}{15\omega^2},\ \ a_5=\frac{\Gamma_5}{24\omega^2},\ \ a_6=\frac{\Gamma_6}{35\omega^2}.\end{aligned} \tag{48}$$

6. Numerical Findings and Analysis

This section compares the analysis of HTS results with the numerical results of literature study in [17]. Figure 2 illustrates the variation in displacement obtained for N/MEMS parameters under vdW forces, in which we demonstrate mathematical software (dotted line), the HTS (black square with straight line), and SRHBM [17] (arrow head with red line). This shows an analysis of the mid-plane deviation of nanobeams obtained numerically using RK4 and qualitatively with HTS and SRHBM.

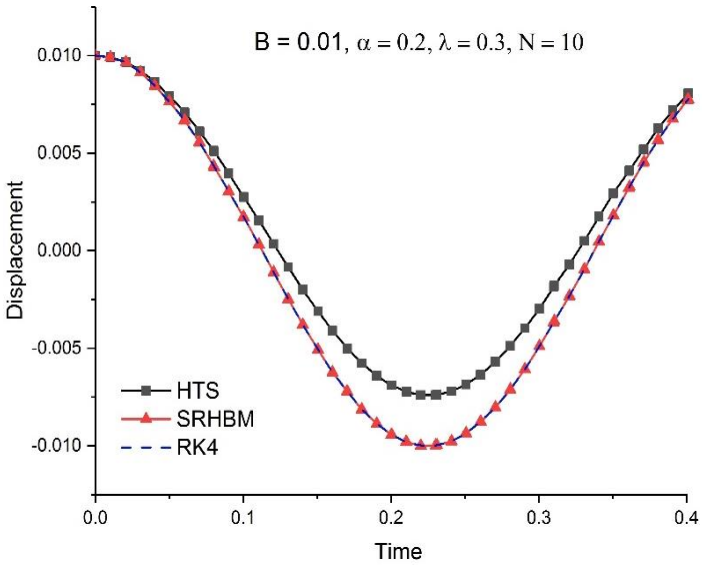

Fig. 2 Comparison of HTS solution with SRHBM and RK4 solution

Fig. 3 presents the error analysis of HTS and SRHBM results over time with various components of identical parameters, in which we demonstrate the HTS results (arrow head with red line), and SRHBM [17] (circle with red line). The parametric values are described to show the efficiency of model.

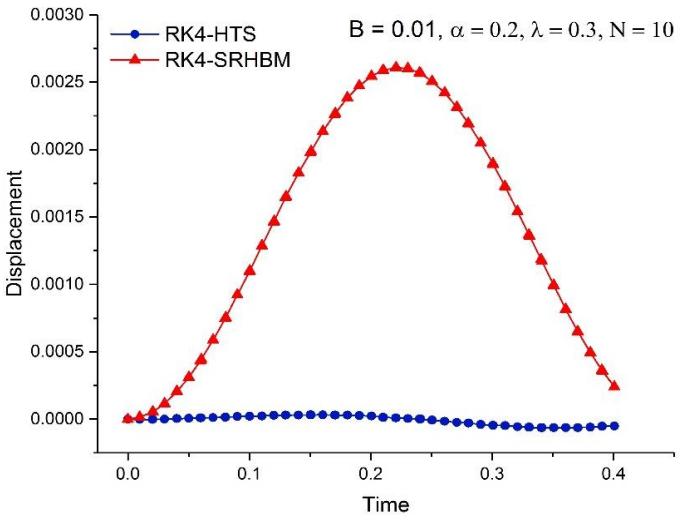

Fig. 3 Error analysis between HTS and SRHBM solutions

Fig. 4 examines the variation in parameters by using our purposed scheme, whereas the other three parameters remain unchanged. The results of the HTS and by using the mathematical software are in agreement at various values of the amplitude parameters.

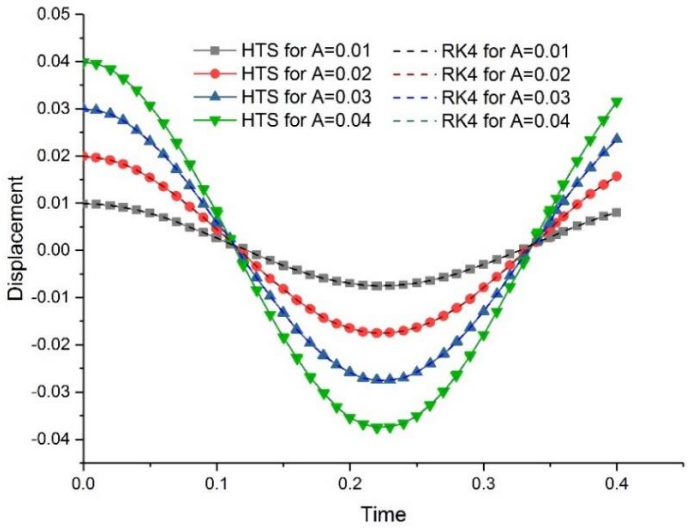

Fig. 4 Effects of amplitude on deflection of nanobeam

Fig. 5 shows the impact of HTS for the significant results of N/MEMS system. Only one parameter is changed, while the other three parameters remain unchanged at α=0, 50, 100, 150.

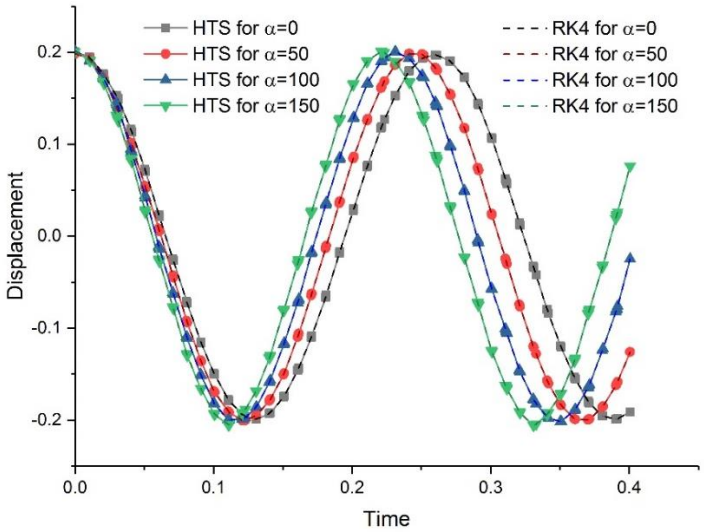

Fig. 5 Effects of gap parameter on deflection of nanobeam

Fig. 6 illustrates the various elements of the problem influenced by HTS solution. The other three remain steady parameters and only one factor is changed at λ=0, 0.3, 0.6, 0.9.

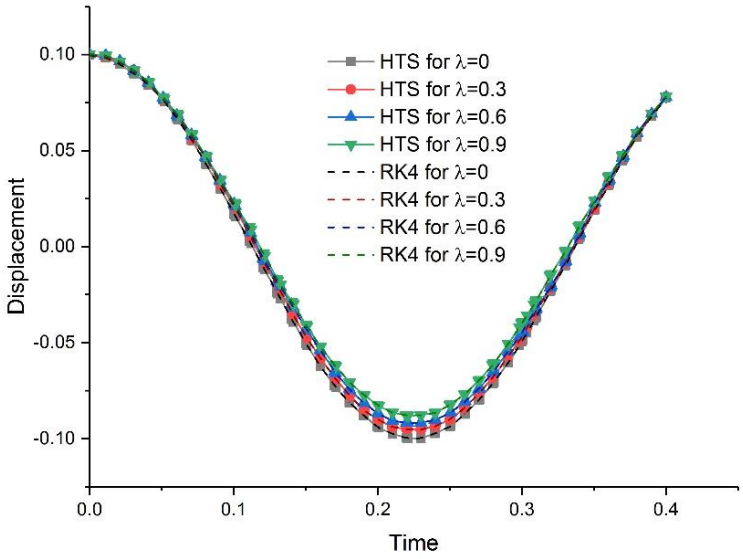

Fig. 6 Effects of parameters on deflection of nanobeam

Fig. 7 highlights the variation of the problem affected by the HTS solution. The other three factors endure constant; only one is changed. The results from HTS and using software are in perfect alignment with the parameter's value N=0, 5, 10, 15. In our graphical

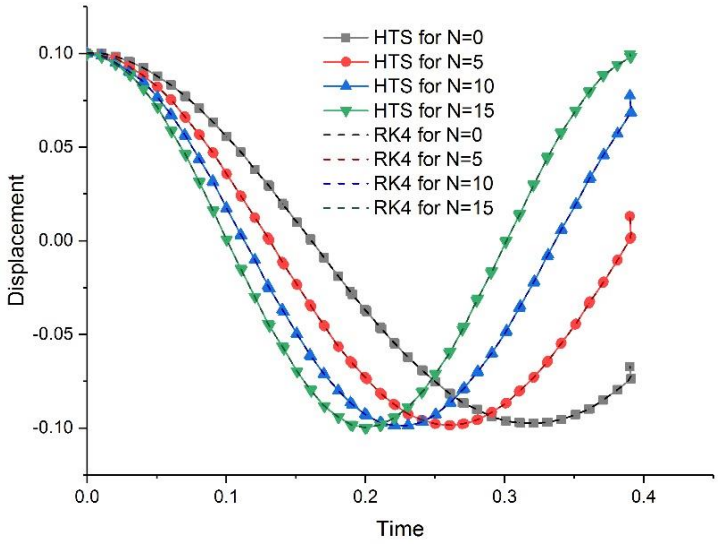

Fig. 7 Effects of axial load parameter on deflection of nanobeam

structure, we can conclude that HTS results have strong agreement for N/MEMS system based on microstructure using vdW forces. In the fundamental oscillation concept, the fact is recognized that the closed orbits illustrated in these phase visuals refer to oscillatory behavior. It is anticipated that significant values exist within the range of parameters that lead to the existence of pull-in solutions.

7. CONCLUSION

This study examined a general oscillation in a highly nonlinear N/MEMS system, which describes the motion of a microbeam under the influence of vdW forces. Our proposed method rapidly converges to results and demonstrates high accuracy, even with the first-order approximation step. The derived results confirm the efficiency of the suggested approach and provide better performance than other techniques. Micro-sensors used for monitoring and controlling vibrations in machinery are a practical application of MEMS in mechanical engineering. This research contributes to our comprehension and improvement of MEMS performance by examining signal stability, energy efficiency, and resilience in severe conditions, which are crucial for dependable, long-term functioning in mechanical domains. In the future research, we intend to expand this scheme to address other nonlinear challenges in N/MEMS systems that incorporate fractal and fractional derivatives.

Acknowledgement: *The authors extend their appreciation to the Deanship of Research and Graduate Studies at King Khalid University for funding this work through Large Research Project under grant number RGP2/297/45.*

REFERENCES

1. Maroufi, M., Fowler, A.G., Moheimani, S.R., 2017, *MEMS for nanopositioning: Design and applications*, Journal of Microelectromechanical Systems, 26(3), pp. 469-500.
2. Faudzi, A.A.M., Sabzehmeidani, Y., Suzumori, K., 2020, *Application of micro-electro-mechanical systems* (*MEMS*) *as sensors: A review*, Journal of Robotics and Mechatronics, 32(2), pp. 281-288.
3. Noormohammadi, N., Asadi, A.M., Mohammadi D.P., Boroomand, B., 2023, *Buckling and free vibration analysis of in-plane heterogeneous nanoplates using a simple boundary method*, Journal of the Brazilian Society of Mechanical Sciences and Engineering, 45(5), 267.
4. Faghidian, S.A., Tounsi, A., 2022, *Dynamic characteristics of mixture unified gradient elastic nanobeams*, Facta Universitatis-Series Mechanical Engineering, 20(3), pp. 539-552.
5. Zhang, Y., Tian, D., Pang, J., 2022, *A fast estimation of the frequency property of the microelectromechanical system oscillator*, Journal of Low Frequency Noise, Vibration and Active Control, 41(1), pp. 160-166.
6. He, C.H., 2022, *A variational principle for a fractal nano/microelectromechanical* (*N/MEMS*) *system*, International Journal of Numerical Methods for Heat & Fluid Flow, 33(1), pp. 351-359.
7. Phi, B.G., Hieu, D.V., Sedighi, H.M., Sofiyev A.H., 2022, Size-dependent nonlinear vibration of functionally graded composite micro-beams reinforced by carbon nanotubes with piezoelectric layers in thermal environments, Acta Mechanica, 233(6), PP. 2249-2270.
8. Aliasghary, M., Mobki, H., Ouakad, H.M., 2022, Pull-in phenomenon in the electrostatically micro-switch suspended between two conductive plates using the artificial neural network, Journal of Applied and Computational Mechanics, 8(4), pp. 1222-1235.
9. Shamsmohammadi, N., Samadi, H., Rahimzadeh, M., Asadi, Z., Ganji, D.D., 2023, *Nano/micro-beam deflections: Investigation of subjected forces and applications*, Physics Open, 17, 100191.
10. Tian, D., He, C.H., 2021, *A fractal micro-electromechanical system and its pull-in stability*, Journal of Low Frequency Noise, Vibration and Active Control, 40(3), pp. 1380-1386.

11. Cho, J.H., Cayll, D., Behera, D., Cullinan, M., 2021, *Towards repeatable, scalable graphene integrated micro-nano electromechanical systems* (*MEMS/NEMS*), Micromachines, 13(1), 27.
12. He, J.H., He, C.H., Qian, M.Y., Alsolami, A.A., 2024, *Piezoelectric biosensor based on ultrasensitive mems system*, Sensors and Actuators A: Physical, 376, 115664.
13. Padha, B., Yadav, I., Dutta, S., Arya, S., 2023, *Recent developments in wearable NEMS/MEMS-based smart infrared sensors for healthcare applications*, ACS Applied Electronic Materials, 5(10), pp. 5386-5411.
14. He, J.H., 1999, *Variational iteration method-a kind of non-linear analytical technique: some examples*, International journal of non-linear mechanics, 34(4), pp. 699-708.
15. Fu, Y., Zhang, J., Wan, L., 2011, *Application of the energy balance method to a nonlinear oscillator arising in the microelectromechanical system* (*MEMS*), Current applied physics, 11(3), pp. 482-485.
16. Sedighi, H.M., Daneshmand, F., Yaghootian, A., 2014, *Application of iteration perturbation method in studying dynamic pull-in instability of micro-beams*, Latin American Journal of Solids and Structures, 11, pp. 1078-1089.
17. Qian, Y., Pan, J., Qiang, Y., Wang, J., 2019, *The spreading residue harmonic balance method for studying the doubly clamped beam-type N/MEMS subjected to the van der Waals attraction*, Journal of Low Frequency Noise, Vibration and Active Control, 38(3-4), pp. 1261-1271.
18. Sedighi, H.M., Shirazi, K.H., 2013, *Vibrations of micro-beams actuated by an electric field via Parameter Expansion Method*, Acta Astronautica, 85, pp. 19-24.
19. Zhang, K., Xie, J., Hao, S., Zhang, Q., Feng, J., 2023, *Exploring nonlinearity to enhance the sensitivity and bandwidth performance of a novel tapered beam micro-gyroscope*, Journal of Sound and Vibration, 562, 117823.
20. Jena, R.M., Chakraverty, S., 2019, *Residual power series method for solving time-fractional model of vibration equation of large membranes*, Journal of Applied and Computational Mechanics, 5(4), pp. 603-615.
21. Song, Q.R., Zhang, J.G., 2024, He-transform: breakthrough advancement for the variational iteration method, Frontiers in Physics, 12, 121411691.
22. Yang, Q., 2023, *A mathematical control for the pseudo-pull-in stability arising in a micro-electromechanical system*, Journal of Low Frequency Noise, Vibration and Active Control, 42(2), pp. 927-934.
23. He, J.H., El-Dib, Y.O., 2020, *Homotopy perturbation method for Fangzhu oscillator*, Journal of Mathematical Chemistry, 58, pp. 2245-2253.
24. Qayyum, M., Oscar, I., 2021, *Least square homotopy perturbation method for ordinary differential equations*, Journal of Mathematics, 2021(1), 7059194.
25. Anjum, N., He, J.H., 2020, *Homotopy perturbation method for N/MEMS oscillators*, Mathematical methods in the applied sciences, https://doi.org/10.1002/mma.6583.
26. He, J.H., He, C.H., Alsolami, A.A., 2023, *A good initial guess for approximating nonlinear oscillators by the homotopy perturbation method*, Facta Universitatis-Series Mechanical Engineering, 21(1), pp. 021-029.
27. Tao, H., Anjum, N., Yang, Y. J., 2023, *The Aboodh transformation-based homotopy perturbation method: new hope for fractional calculus*, Frontiers in Physics, 11, 1168795.
28. Niu, J.Y., He, C.H., Alsolami, A.A., 2024, *Symmetry-breaking and pull-down motion for the Helmholtz-Duffing oscillator*, Journal of Low Frequency Noise, Vibration and Active Control, 43(1), pp. 263-271.
29. Bulut, H., Baskonus, H.M., Belgacem, F.B.M., 2013, *The analytical solution of some fractional ordinary differential equations by the Sumudu transform method*, Abstract and Applied Analysis, 2013(1), 203875.
30. Patel, T., Meher, R., 2017, *Thermal analysis of porous fin with uniform magnetic field using Adomian decomposition Sumudu transform method*, Nonlinear Engineering, 6(3), pp. 191-200.
31. Sahni, M., Parikh, M., Sahni, R., 2021, *Sumudu transform for solving ordinary differential equation in a fuzzy environment*, Journal of Interdisciplinary Mathematics, 24(6), pp. 1565-1577.
32. Nadeem, M., Alsayaad, Y., 2024, *Analytical study of one dimensional time fractional Schrödinger problems arising in quantum mechanics*, Scientific Reports, 14(1), 12503.
33. Askari, A.R., Tahani, M., Moeenfard, H., 2017, *A frequency criterion for doubly clamped beam-type N/MEMS subjected to the van der Waals attraction*, Applied Mathematical Modelling, 41, pp. 650-666.
34. He, C.H., El-Dib, Y.O., 2022, *A heuristic review on the homotopy perturbation method for non-conservative oscillators*, Journal of Low Frequency Noise, Vibration and Active Control, 41(2), pp. 572-603.
35. He, C.H., Amer, T.S., Tian, D., Abolila, A.F., Galal, A.A., 2022, *Controlling the kinematics of a spring-pendulum system using an energy harvesting device*, Journal of Low Frequency Noise, Vibration and Active Control, 41(3), pp. 1234-1257.
36. He, C.H., Tian, D., Moatimid, G.M., Salman, H.F., Zekry, M.H., 2022, *Hybrid Rayleigh-van der pol--duffing oscillator: stability analysis and controller*, Journal of Low Frequency Noise, Vibration and Active Control, 41(1), pp. 244-268.

APPENDIX:

The components defined by Eq. (29) are obtained as follows:

$$q_0 = \int_0^1 \varsigma^2 d\varphi,\ q_1 = -3\int_0^1 \varsigma^3 d\varphi,\ q_2 = 3\int_0^1 \varsigma^4 d\varphi,\ q_3 = -\int_0^1 \varsigma^5 d\varphi,\ q_4 = -\lambda\int_0^1 \varsigma\, d\varphi,$$

$$q_5 = \int_0^1 (\varsigma\varsigma'''' - N\varsigma\varsigma'')\, d\varphi,\ q_6 = \int_0^1 (-3\varsigma^2\varsigma'''' + 3N\varsigma^2\varsigma'')\, d\varphi,$$

$$q_7 = \int_0^1 (3\varsigma^3\varsigma'''' - 3N\varsigma^3\varsigma'')\, d\varphi - \alpha\int_0^1 \varsigma\varsigma'' d\varphi \int_0^1 \varsigma'^2 d\varphi,$$

$$q_8 = \int_0^1 (-\varsigma^4\varsigma'''' + N\varsigma^4\varsigma'')\, d\varphi + 3\alpha\int_0^1 \varsigma^2\varsigma'' d\varphi \int_0^1 \varsigma'^2 d\varphi,$$

$$q_9 = -3\alpha\int_0^1 \varsigma^3\varsigma'' d\varphi \int_0^1 \varsigma'^2 d\varphi,\quad q_{10} = \alpha\int_0^1 \varsigma^4\varsigma'' d\varphi \int_0^1 \varsigma'^2 d\varphi.$$

where $\varsigma(\varphi)=\sin(\pi\varphi)$.